Emerg Radiol (2015) 22:307–314
DOI 10.1007/s10140-014-1274-5

PICTORIAL ESSAY

MDCT of the hand and wrist: beyond trauma

Shivani Ahlawat · Frank M. Corl · Elliot K. Fishman · Laura M. Fayad

Received: 14 July 2014 / Accepted: 26 September 2014 / Published online: 10 October 2014

Abstract High-resolution multidetector computed tomography (MDCT) has played a pivotal role in assessing patients following trauma; however, recent advancements in technology including dual-energy CT, as well as multiplanar and three-dimensional (3D) capabilities, are expanding the potential clinical applications of CT to include nontraumatic pathologies. This article will review optimal technical parameters for the creation of MDCT and 3DCT images and illustrate the imaging capabilities of 3DCT imaging for demonstrating nontraumatic hand and wrist pathology.

Keywords Computed tomography · Multiplanar reconstructions · 3DCT · Hand · Wrist

Introduction

CT imaging has played a central role in assessing patients following musculoskeletal trauma, especially for the evaluation of radiographically occult fractures in the hand and wrist [1–4]. However, the indications and utility of CT are expanding, and multidetector computed tomography (MDCT) and three-dimensional (3D) CT imaging are useful techniques for the demonstration of nontraumatic hand and wrist abnormalities of the soft tissues. Table 1 provides a brief overview of indications for CT imaging of nontraumatic abnormalities of the hand and wrist. Technical optimization for the creation of 2D and 3DCT images, including optimal CT acquisition parameters and 3D reconstruction algorithms, will be reviewed. The added value of 3DCT imaging in the assessment of nontraumatic hand and wrist pathology will be illustrated in the setting of infectious, neoplastic, metabolic, vascular, and congenital disorders.

S. Ahlawat (✉) · F. M. Corl · E. K. Fishman · L. M. Fayad
The Russell H. Morgan Department of Radiology & Radiological Science, The Johns Hopkins University School of Medicine, 600 North Wolfe Street, Baltimore, MD 21287, USA
e-mail: sahlawa1@jhmi.edu

F. M. Corl
e-mail: fcorl1@jhmi.edu

E. K. Fishman
e-mail: efishman@jhmi.edu

L. M. Fayad
e-mail: lfayad1@jhmi.edu

CT acquisition and postprocessing algorithms

MDCT allows for multiplanar reformations (MPR) and 3D depiction via a single acquisition in any plane. Shaded surface rendering (SSR), a method of 3D volumetric image reconstruction, does not use all the information obtained at the time of acquisition to create the image and is limited to displaying fractures on the surface of bone. Hence, for nontraumatic hand and wrist abnormalities, volume rendering (VR) is the preferred 3D reconstruction algorithm as it utilizes the entire spiral CT dataset in the reconstruction, and thus conveys more information than SSR. VR images may be displayed in any projection and rendered to display any particular tissue [5, 6]. A contrast material is administered in the setting of infection, inflammation, neoplasm, or vascular disorders.

With the advent of dual-energy CT, metabolic disorders of the hand and wrist such as gout can be characterized. With dual-energy CT, two X-ray tubes with a peak kilovoltage of 80 and 140 kVp are simultaneously used to acquire two sets of images from a region of interest. Comparing the material-specific differences in attenuation on the two energy acquisitions allows differentiation of the chemical composition of the scanned area.

Table 1 Indications for CT of the hand and wrist

CT technique	Indication
Noncontrast CT	1. Skeletal neoplasms
	A. Determination of tumor extent (if MRI is contraindicated)
	B. Characterization of skeletal lesions (mineralization, matrix composition, endosteal scalloping, periosteal reaction, pattern of bone marrow destruction)
	2. Osteomyelitis (identification of erosions, periosteal reaction, sinus tracts, sequestra, involucrum)
Contrast-enhanced CT	1. Soft tissue neoplasms
	A. Determination of tumor extent (if MRI is contraindicated)
	B. Characterization of soft tissue mass (mineralization pattern, soft tissue density, relationship to adjacent bone, tumor vascularity)
Contrast-enhanced CT	1. Vascular disorders (assessment of morphologic changes in arteries with disease)
	2. Soft tissue infection (identification of abscess, pyomyositis, fasciitis)
Dual-energy CT (1)	1. Characterization of mineralization (distinguishing urate from other minerals)
	2. Assessment of gout (detection and quantification of tophi)

Although CT has been used routinely in the setting of trauma for assessment of radiographically occult fractures as well as postoperative healing, other common indications for CT are listed above

Nontraumatic abnormalities of the hand and wrist

Infections

Hand infections can vary from routine problems treated with oral antibiotics, immobilization, and limited incision and drainage to catastrophic surgical emergencies resulting in the significant compromise of hand function. In Friedrich's and Imahara's retrospective review of hand infections over an 11-year period, tenosynovitis was the most common type of infection, comprising 67.3 % of the patients, and soft tissue abscess and septic arthritis comprised the remaining 28.9 %. The infectious processes in the hand and wrist can be categorized into superficial infections (arising from the skin and subcutaneous tissues superficial to the tendons) and deep infections (located deep to the tendon sheaths). Superficial hand infections include cellulitis, lymphangitis, paronychia, pulp space infections, herpetic whitlow, subcutaneous abscesses, and web space abscesses and can be treated nonsurgically; deep hand infections involve synovial space infections, deep fascial space infections, septic arthritis, and necrotizing fasciitis and are often surgical emergencies [7, 8].

It is important for the radiologist to understand the potential spaces of the hand and wrist where infections can be located. The hand has three anatomically defined potential spaces and the forearm has one potential space (Fig. 1). These septated spaces lie between muscle fascial planes and include the thenar, midpalmar, and hypothenar spaces in the hand and Parona's space in the forearm. There are three more superficial spaces in the hand: the dorsal subcutaneous space, the dorsal subaponeurotic space, and the interdigital web space. The administration of a contrast material is essential to diagnose a loculated fluid collection in the superficial, subcutaneous, or interdigital web spaces and differentiate that from a fluid collection in the deep synovial or fascial spaces. Contrast is also useful for diagnosing fasciitis, pyomyositis, and synovitis.

Subcutaneous abscesses of the hand can occur on either the palmar or dorsal aspects of the hand, whereas an interdigital web space infection is a subcutaneous web space abscess that can involve the palmar and dorsal aspects simultaneously. A palmar subcutaneous abscess is typically localized due to fibrous septae anchoring the palmar skin limit; however, a

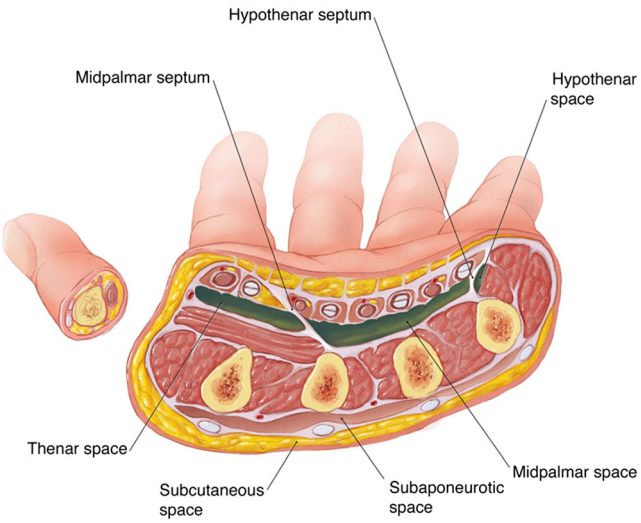

Fig. 1 Potential spaces of the hand and wrist. The hand has three anatomically defined potential spaces and the forearm has one potential space. These septated spaces (identified by the *color green*) lie between muscle fascial planes and include the thenar, midpalmar, and hypothenar spaces in the hand and Parona's space in the forearm. There are three more superficial spaces in the hand: the dorsal subcutaneous space, the dorsal subaponeurotic space, and the interdigital web space

dorsal subcutaneous abscess has the potential to spread into the dorsal subcutaneous space, which is superficial to the extensor tendons, and the dorsal subaponeurotic space, which is deep to the extensor tendons (Fig. 2). Aspiration and decompression of a subcutaneous abscess can be adequate, although a complex dorsal subcutaneous abscess may require extensive debridement. An interdigital web space abscess requires a combined palmar and dorsal surgical approach for adequate drainage and debridement.

Deep hand infections are deep to the tendon sheaths and include synovial space infections, deep fascial space infections, septic arthritis, and necrotizing fasciitis. Synovial space infections including infectious tenosynovitis require surgical intervention. Infections into the deep fascial spaces occur following a penetrating injury in most cases and, occasionally, as an extension from a subcutaneous abscess or adjacent pyogenic flexor tenosynovitis. Deep fascial space infections with involvement of the thenar, midpalmar, and hypothenar spaces are surgical emergencies. Surgical treatment of necrotizing fasciitis consists of wide debridement of skin, subcutaneous tissue, fascia, and any necrotic muscle. The imaging findings of necrotizing fasciitis include thickened fascia, deep fascial fluid, extension of edema into intermuscular septa, and lack of enhancement of the fascia, showing the value of contrast-enhanced scans [9]. The presence of gas in the subcutaneous tissues due to gas-forming bacteria can also aid in the diagnosis, but this finding is not always present.

CT features of septic arthritis include joint effusion, synovitis, periarticular erosions, as well as periarticular edema (Fig. 3). Studies have demonstrated that septic wrists drained more than 16 h after presentation had worse results compared with those surgically treated within 10 h [10]. Finally, CT features of bacterial osteomyelitis include soft tissue swelling, periosteal reaction, focal cortical erosions, and regions of low attenuation in the cavity or trabecular coarsening. An extramedullary fat-fluid level in the absence of trauma is a rare but specific sign for osteomyelitis [9]. CT is considered superior to MR imaging in the setting of chronic osteomyelitis for the demonstration of cortical destruction and gas, and sequestra are better detected with CT [9]. MDCT with 3D reconstructions are a readily available modality in the emergency setting; the images can be rapidly acquired and reformatted to analyze compartmental anatomy in all dimensions and provide vital information for surgical planning.

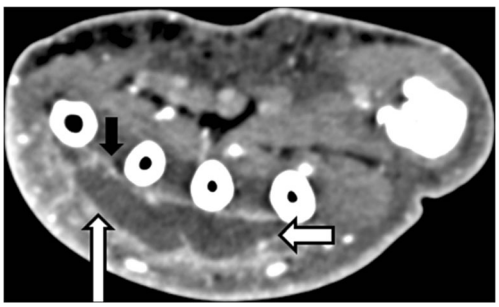

Fig. 2 A 43-year-old man with history of intravenous drug use presenting with superficial hand infection. The dorsal hand cellulitis has extended into the dorsal subaponeurotic space (*short white arrow*) with a loculated fluid collection located deep to the extensor tendons (*long white arrow*). The volar border of this collection is comprised of dorsal interosseous muscles (*short black arrow*). The patient underwent emergent incision and drainage of dorsal hand abscess. Intraoperatively, gross purulence was encountered superficial and deep to the extensor retinaculum. Gram stain and cultures from the hand revealed moderate polymorphonuclear leukocytes with gram-positive cocci found to be *Streptococcus viridans*

Fig. 3 A 45-year-old man with septic arthritis of the thumb interphalangeal joint. Note the periarticular cortical destruction (*arrow*) consistent with septic arthritis

Neoplasms

CT provides adequate anatomic detail for assessing the soft tissues, although its contrast resolution is inferior to that of MRI. The most common soft tissue lesion in the hand and wrist is a ganglion, accounting for 50–70 % of the lesions [11]. Although a ganglion can develop at any joint or tendon sheath, the most common location in the wrist is the dorsal aspect of the wrist adjacent to the scapholunate ligament while the most common locations in the hand include the flexor tendon sheaths and distal interphalangeal joints [11]. Measurements of CT Hounsfield units of a lesion can provide clues to the internal composition, particularly for diagnosing a cyst or lipoma (Fig. 4). Lesions containing fluid include simple cysts or periarticular ganglia, as well as cystic-appearing solid masses that are distinguished by the administration of an IV contrast material (Fig. 5).

After a ganglion, a giant cell tumor of the tendon sheath and epidermal inclusion cyst are the second and third most common lesions of the hand and wrist. Epidermal inclusion cysts result from penetrating trauma, with deposition of keratin-producing epithelial cells into the soft tissues. When large, an inclusion cyst frequently will cause pressure erosion

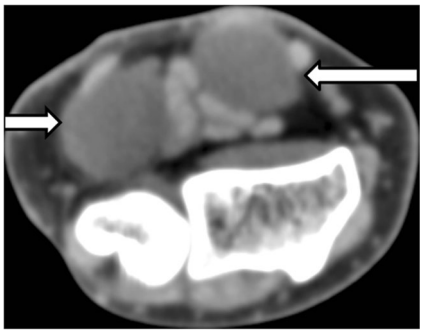

Fig. 4 A 52-year-old woman with neurofibromatosis type II. The axial CT image shows an ulnar (*short arrow*) as well as median (*long arrow*) nerve schwannoma. Although the CT imaging appearance is not diagnostic, the lack of fluid or fat attenuation which would suggest ganglion or lipoma as well as absence of mineralization does exclude some diagnostic possibilities

of the underlying phalanx. Foreign body granulomas may be difficult to distinguish clinically from an epidermal inclusion cyst, especially when it is on the tactile surface of a digit; however, CT imaging can aid in differentiation when a foreign material is identified. CT is helpful in characterizing the mineralization patterns of soft tissue masses that can be difficult to detect on MR imaging or radiography [12]. CT, especially 3DCT, is excellent in revealing the effects of a mass on the adjacent osseous structures [13]. Hence, CT may be useful for preoperative planning, especially when MRI is not available or contraindicated.

CT also provides useful information for the characterization of skeletal lesions by observing the pattern of bone marrow destruction, periosteal reaction, mineralization, density of the lesion (ex: lipid in intraosseous lipoma), or degree of endosteal scalloping [12]. When tumors generate an osteoid or chondroid extracellular matrix, the resultant distinctive mineralization patterns may suggest a histologic diagnosis (Fig. 6). CT assessment of an intralesional matrix is particularly helpful in the hand and wrist as the most commonly occurring bone tumor at this site is an enchondroma. Worrisome imaging features of an enchondroma such as increasing size, endosteal scalloping, and increasing unmineralized component can also be readily detected via CT imaging. Soft tissue and skeletal malignancy within the hand and wrist are exceedingly rare, though CT can aid in detection of complicating features such as pathological fracture. Mori et al., in their retrospective review of 32 patients with bone lesions, concluded that MDCT provided additional and more comprehensive information than MRI and radiography for the preoperative assessment of musculoskeletal masses with respect to the presence of mineralization and cortical involvement [14].

Fig. 5 A 64-year-old man with incompletely resected fibrosarcoma. The VR 3DCT image shows hyperemia and vascular encasement of the volar soft tissues of the proximal long finger (*arrow*)

Fig. 6 A 15-year-old boy with osteoid osteoma of the ring finger proximal phalanx. Note the marked cortical thickening of the proximal phalanx seen on coronal MPRs. Also, the coronal image shows a subtle calcified nidus (*arrow*) in the lucent lesion

Metabolic diseases

The utility of dual-energy CT has been extrapolated from its use in characterizing uric acid renal stones in body CT to distinguish urate-containing gouty tophi from dystrophic calcification. Gout is a disorder of urate metabolism that leads to formation of urate crystals. Urate crystals can be deposited under the skin, in joints, and within tendon sheaths as gouty tophi, which cause an intense inflammatory process. Both radiography and conventional diagnostic CT show increased attenuation within urate crystals and calcium-containing mineralization; however, dual-energy CT can distinguish urate crystals from other deposits at a symptomatic site (Fig. 7). In addition, dual-energy CT may depict subclinical urate crystal deposition at asymptomatic sites that have been included in the imaging field; this enables the clinician to treat gout before irreversible joint damage occurs [15, 16]. In addition, CT is more sensitive in the detection of subtle erosions in the setting of inflammatory arthropathy such as rheumatoid arthritis [17].

CT is also useful for detecting mineralization in chondrocalcinosis (associated with many disorders including pseudogout or calcium pyrophosphate dehydrate (CPPD) arthropathy) as well as periarticular deposits of calcium due to metastatic calcification commonly seen in chronic renal failure. Pseudogout is characterized by self-limited acute or subacute attacks of arthritis that closely resemble gout. The presence of chondrocalcinosis and imaging findings of degenerative arthritis in a joint not typically affected by primary osteoarthritis aid in the diagnosis of CPPD arthropathy. MDCT readily demonstrates subtle mineralization in the hyaline and fibrocartilage as well bursae and tendons associated with chondrocalcinosis. In addition, CT can also show the sheetlike patterns of calcification in the skin, subcutaneous tissue, and fascial planes (calcinosis universalis) that can be present with autoimmune connective tissue disorders, such as polymyositis or dermatomyositis or trauma such as electrocution (Fig. 8).

Vascular disorders

Vascular disorders of the hand and wrist consist of diverse conditions that can be classified as vaso-occlusive disease, vasospastic conditions, compressive vascular disease, congenital vascular disease, congenital vascular malformation, vascular neoplasm, and venous occlusive disease. CT, specifically CT angiography, plays an important role in the assessment of the vasculature in the setting of trauma for the detection of vaso-occlusive and vasospastic conditions such as pseudoaneurysms, arterial dissection, and active hemorrhage. However, CT angiography may also aid in the characterization of soft tissue masses, by revealing arterial or venous lesion vascularity, which is characteristic of certain tumors or vascular malformations [12].

Vascular malformations can be categorized based on low or high flow. Low-flow vascular malformations are characterized by slow flow with resultant pooling of blood and contrast material. High-flow vascular malformations, such as arteriovenous fistulas and arteriovenous malformations, have large feeding arteries in addition to draining vessels (Fig. 9). It is important to remember that both large low-flow malformations and noninvoluting hemangiomas can also have large feeding and draining vessels. Another utility of CT is in its depiction of phleboliths, characteristic features of vascular malformations.

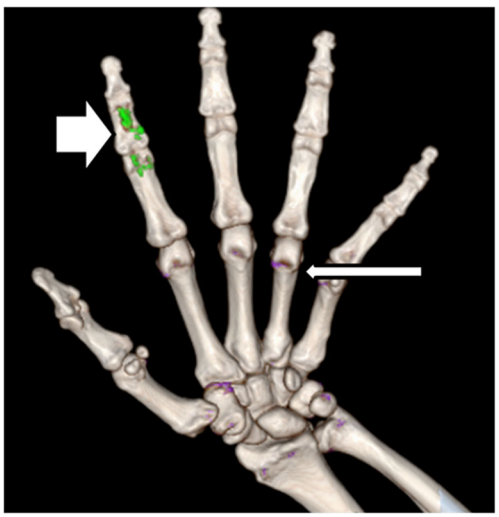

Fig. 7 A 50-year-old man with gout. A color-coded composition 3DCT image obtained with postprocessing techniques by using data from dual-energy CT shows uric acid deposits (*green* areas—*short arrow*) compatible with uric acid in this patient with gout. These uric acid deposits are distinct from periarticular, dystrophic calcification (*purple—long arrow*)

Fig. 8 A 45-year-old woman with prior history of electrocution. MDCT shows radial soft tissue calcifications (*arrows*) related to prior electrocution in addition to arteriosclerotic vascular calcification

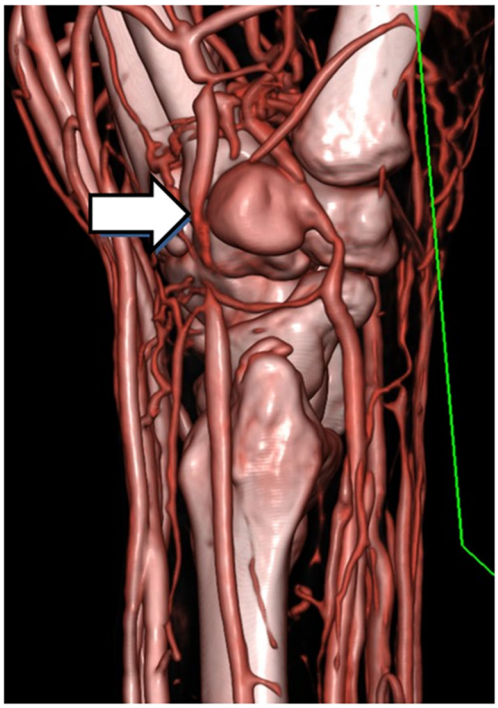

Fig. 9 A 23-year-old man with known history of vascular malformation. MDCT angiography demonstrates a high-flow arteriovenous malformation with a large, partially thrombosed pseudoaneurysm (*arrow*)

Foreign bodies

A foreign body within the hand or wrist can cause immediate or chronic complications such as infection, inflammation, a tumor-like granuloma, or tenosynovitis. The detection of retained foreign bodies can be extremely challenging in the chronic setting, without definite antecedent penetrating trauma and nonspecific symptoms of pain and/or swelling related to a foreign body granuloma.

Nonradiopaque foreign bodies such as wooden fragments or splinters can be difficult to detect on radiography alone [18]. In addition, very small foreign bodies can be a challenge on MRI as well as sonography. CT has a sensitivity ranging from 65 % (for a foreign body <0.06 mm^3) to 100 % (for foreign bodies >0.06 mm^3) [19]. CT provides precise compartmental anatomy for delineation of the extent of involvement by a foreign body, similar in importance to identifying the exact site of compartmental infection (Fig. 10). Conventional CT can detect retained foreign bodies in the acute postoperative period for years after the initial surgery. Yang et al. studied the added value of 3DCT in radiopaque foreign body retrieval from the soft tissues in 435 patients who underwent radiography and contrast-enhanced 3DCT [20]. The authors found that 3DCT more accurately revealed foreign body size, shape, number, distribution, and relationship to the adjacent vasculature. Although other modalities such as radiographs and ultrasound can identify foreign body complications such as arteriospasm, vascular laceration, and pseudoaneurysm, 3DCT was more accurate for making optimal management decisions.

Fig. 10 A 26-year-old man with hand and wrist foreign body. Sagittal MDCT elegantly displays the bullet fragments in addition to a partially lacerated ring finger extensor tendon (*arrow*)

Fig. 11 A 20-year-old woman with Madelung deformity. 3DCT demonstrates typical skeletal findings of Madelung with discongruent distal radioulnar joint, medially foreshortened radius and relative overgrowth of the ulna, and V-shaped proximal carpal row (*arrow*)

Congenital disorders

Congenital disorders of the hand encompass myriad deformities, all of which carry different functional and cosmetic implications for the patient and parents. Congenital hand anomalies are estimated to occur in 10 % of children born with congenital abnormalities [11]. They can be conceptualized as disorders of formation, failure of differentiation, duplication, overgrowth syndromes, undergrowth syndromes, constriction ring syndromes, and generalized skeletal abnormalities. The most commonly encountered anomalies of the hand are syndactyly, polydactyly, congenital amputations, camptodactyly, clinodactyly, and radial clubhand [11]. Typically, congenital disorders of the hand and wrist are detected via a prenatal ultrasound and characterized by postnatal radiography. MDCT has the ability to comprehensively demonstrate the spatial arrangement of the bones as well as the anatomy of the soft tissue structures, especially in the preoperative setting [21]. Madelung deformity is a rare congenital anomaly of the wrist caused by asymmetric growth at the distal radial physis secondary to a partial ulnar-sided arrest (Fig. 11). It is characterized by a growth disturbance in the palmar and ulnar portions of the physis, resulting in a 3D complex radial deformity, that is, an exaggerated tilt of the articular surface in the ulnopalmar direction and diaphyseal bowing. The utility of 3DCT imaging for preoperative planning of cylindrical corrective osteotomy of the distal radius has been described using 3D surgical guides based on a preoperative CT scan [22].

Conclusions

High-resolution MDCT, in concert with 3DCT, is a useful technique for the demonstration of hand and wrist nontraumatic soft tissue abnormalities. The MPR and 3D capabilities of MDCT, along with the advent of dual-energy CT, are important tools for the characterization of soft tissue pathologies of the hand and wrist and complement the information offered by other cross-sectional modalities, including ultrasound and MRI.

Grants and disclosures Laura M. Fayad received support from SCBT/MR (2004), GERRAF (2008–2010) and Siemens Medical Systems (2011–2012) for the study of MR spectroscopy and Johns Hopkins Sarcoma Grant (2012).

Conflict of interest The authors declare that they have no conflict of interest.

References

1. Welling RD, Jacobson JA, Jamadar JA, Chong S, Caoili RM, Jemson PJ (2008) MDCT and radiography of wrist fracture: radiographic sensitivity and fracture patterns. AJR 190:10–16
2. Harness NG, Ring D, Zurakowski D, Harris GJ, Jupiter JB (2006) The influence of three-dimensional computed tomography reconstructions on the characterization and treatment of distal radial fractures. J Bone Joint Surg Am 88:1315–1323
3. Cole RJ, Bindra RR, Evanoff BA, Gilula LA, Yamaguchi K, Gelberman RH (1997) Radiographic evaluation of osseous displacement following intra-articular fractures of the distal radius: reliability of plain radiography versus computed tomography. J Hand Surg [Am] 22:792–800
4. Rozental TD, Bozentka DJ, Katz MA, Steinberg DR, Beredjiklian PK (2001) Evaluation of the sigmoid notch with computed tomography following intra-articular distal radius fracture. J Hand Surg 26A:244–251
5. Kuszyk BS, Heath DG, Bliss DF, Fishman EK (1996) Skeletal 3-D CT: advantages of volume rendering over surface rendering. Skelet Radiol 25:207–214
6. Ney DR, Fishman EK, Kawashima A, Robertson DD Jr, Scott WW Jr (1992) Comparison of helical and serial CT with regard to three-dimensional imaging of musculoskeletal anatomy. Radiology 185:865–869
7. Franko OI, Abrams RA (2013) Hand infections. Orthop Clin N Am 44:625–634
8. Imahara SD, Friedrich JB (2010) Community-acquired methicillin-resistant Staphylococcus aureus in surgically treated hand infections. J Hand Surg [Am] 35:97–103
9. Fayad LM, Carrino JA, Fishman E (2007) Musculoskeletal infection: role of CT in the emergency department. RadioGraphics 27:1723–1736
10. Rashkoff ES, Burkhalter WE, Mann RJ (1983) Septic arthritis of the wrist. J Bone Joint Surg Am 65:824–828
11. Davies MA, Grainger AJ, James SJ (2013) Imaging of the hand and wrist: techniques and applications. Springer, Heidlerberg
12. Subhawong TK, Fishman EK, Swart JE, Carrino JA, Attar S, Fayad LM (2010) Soft-tissue masses and masslike conditions: what does CT add to diagnosis and management? AJR 194:1559–1567
13. Li Y, Zheng Y, Lin J, Cai A, Zhou X, Wei X, Cheng Y, Liu G (2013) Evaluation of the relationship between extremity soft tissue sarcomas and adjacent major vessels using contrast-enhanced multidetector CT and three-dimensional volume-rendered CT angiography: a preliminary study. Acta Radiol 54:966–972
14. Mori T, Fujii M, Akisue T, Yamamoto T, Kurosaka M, Sugimura K (2005) Three-dimensional images of contrast-enhanced MDCT for preoperative assessment of musculoskeletal masses: comparison with MRI and plain radiographs. Radiat Med 23:398–406
15. Desai MA, Peterson JJ, Garner JJ, Kransdorf MJ (2011) Clinical utility of dual-energy CT for evaluation of tophaceous gout. Radiographics 31:1365–1375. doi:10.1148/rg.315115510
16. Chen CK, Yeh LR, Pan H, Yang CF, Lu YC, Wang JS, Resnick D (1999) Intra-articular gouty tophi of the knee: CT and MR imaging in 12 patients. Skelet Radiol 28:75–80
17. Canella C, Philippe P, Pansini V, Salleron J, Flipo RM, Cotten A (2011) Use of tomosynthesis for erosion evaluation in rheumatoid arthritic hands and wrists. Radiology 258:199–205
18. Anderson MA, Newmeyer WL, Kilgore ES (1982) Diagnosis and treatment of retained foreign bodies in the hand. Am J Surg 144:63–67

19. Mester V, Kuhn F (2002) Intraocular foreign bodies. Ophthalmol Clin N Am 15:235–242
20. Yang XJ, Xing GF, Shi CW, Li W (2013) Value of 3-dimensional CT virtual anatomy imaging in complex foreign body retrieval from soft tissues. Korean J Radiol 14: 269–277
21. Holten IW, Smith AW, Isaacs JI, Moore MH, David DJ (1997) Imaging of the Apert syndrome hand using three-dimensional CT and MRI. Plast Reconstr Surg 99:1657–1680
22. Imai Y, Miyake J, Okada K, Murase T, Yoshikawa H, Moritomo H (2013) Cylindrical corrective osteotomy for Madelung deformity using a computer simulation: case report. J Hand Surg [Am] 38:1925–1932